

A model for the early COVID-19 outbreak in China with case detection and behavioural change

Julien Arino¹, Khalid El Hail^{2,*}, Mohamed Khaladi³, Aziz Ouhinou²

¹Department of Mathematics

University of Manitoba, Winnipeg, Manitoba, Canada

julien.arino@umanitoba.ca  0000-0001-6409-5027

²Department of Mathematics, Faculty of Sciences and Techniques,

University of Sultan Moulay Slimane, Beni-Mellal, Morocco

elhail.kha@gmail.com  0000-0001-5166-9386

a.ouhinou@usms.ma  0000-0002-0206-4935

³Laboratory of Mathematics and Population Dynamics – UMMISCO,

Faculty of Sciences Semlalia, Cadi Ayyad University, Marrakech, Morocco

khaladi@uca.ac.ma  0000-0002-7703-5637

Received: November 5, 2022, Accepted: December 20, 2022, Published: January 27, 2023

Abstract: We investigate a model of the early stage of the COVID-19 epidemic comprising undetected infected individuals as well as behavioural change towards the use of self-protection measures. The model is fitted to China data reported between 22 January and 29 June 2020. Using fitting results, we then consider model responses to varying screening intensities.

Keywords: COVID-19, Behavioural Change, Screening Intensity, Protective Measures

I. INTRODUCTION

At the time of writing, the first known COVID-19 human case is one with onset on 8 December 2019, in Wuhan, China [1, 2], although there is evidence that the disease have been spreading earlier; see [3] for a timeline of early spread. On 20 January 2020, studies confirmed human-to-human transmission through respiratory droplets [4]. There is now an unprecedentedly large body of work on the worldwide COVID-19 outbreak; however, many epidemiological features such

as *per capita* transmissibility, screening and disease-related death rates are still ambiguous and, to a large extent, seem quite dependent on the location under consideration, with outbreak intensities varying greatly from country to country. Parameters may vary from region to region depending, for instance, on control measures taken by policymakers, availability of personal protective equipment, hospitalisation, demographic pyramid, life activities and cultural aspects.

Many works consider the early spread of COVID-19 in China, which at the start of the pandemic had the most data since it had the most cases; the list is far too extensive to detail here and we list just a few. In [5], the authors estimated the basic reproduction number to be up to $\mathcal{R}_0 = 3.58$ at the beginning of the outbreak in China. Using the official counts of confirmed cases, \mathcal{R}_0 was suggested in [6] to be on average 4.6, and, by assuming presymptomatic and mildly symptomatic infectious individuals to be twenty or forty times the reported number of infected cases, the mean of \mathcal{R}_0 was

Copyright: © 2022 Julien Arino, Khalid El Hail, Mohamed Khaladi, Aziz Ouhinou. This article is distributed under the terms of the Creative Commons Attribution License (CC BY 4.0), which permits unrestricted use, distribution, and reproduction in any medium, provided the original author and source are credited.

*Corresponding author

Citation: Julien Arino, Khalid El Hail, Mohamed Khaladi, Aziz Ouhinou,

A model for the early COVID-19 outbreak in China with case detection and behavioural change,

Biomath 11 (2022), 2212207, <https://doi.org/10.55630/j.biomath.2022.12.207>

estimated to be 3.2 or 2.6, respectively; daily infection mortality and recovery rates were also estimated. In addition, in the early stage of the COVID-19 epidemic in China, [1] suggested \mathcal{R}_0 to be approximately 2.2 and the incubation period to have a mean of 5.2 days.

Because infection severity differs greatly in infected individuals, some individuals are infectious while presymptomatic. Together with asymptomatic infections, this means that some individuals may have “evaded” screening, despite contributing to the spread of the disease [6–9]. Besides isolating detected active cases and their known immediate contacts, healthcare authorities worldwide did their best to educate the population about COVID-19 severity, its mode of transmission and convince people to use all available preventive measures.

Accordingly, in this work we take into consideration the population response to education campaigns. We use a system of differential equations to model the COVID-19 epidemic with, including burden-dependent behavioural change. We calibrate some of the parameters so that the model fits the COVID-19 data in China from 22 January until 29 June 2020.

This article is organised as follows. In Section II, the mathematical model of COVID-19 transmission is derived. Section III presents numerical results, which are then discussed further in Section IV.

II. MATHEMATICAL MODELLING

The mathematical model considered in this paper comprises seven epidemiological compartments, S , E , I_S , I_E , J_D , J_T and R , as well as an auxiliary variable, A , used to account for awareness of the disease. The flow diagram is shown in Figure 1; let us elaborate on this structure.

S are susceptible individuals in the classical sense, while E denotes educated susceptible individuals using self-protective measures against the infection. Infected individuals are divided into four compartments. I_S and I_E are, respectively, non-educated and educated undetected *infectious* individuals; individuals in both of these compartments who get screened move, upon detection, into the isolation compartment J_D , where they wait for recovery or a potential hospitalisation [10]. If their infection goes undetected, upon recovery or death, they progress directly to the removed compartment. The fourth infected compartment, J_T , contains infected cases who are under treatment in hospital. Both J_D and J_T are isolated and as a consequence, they are not infectious to others. The compartment R is for

Table I: State variables.

Variable	Definition
S	Susceptible individuals
E	Educated susceptible individuals
I_S	Undetected infectious non-educated individuals
I_E	Undetected infectious educated individuals
J_D	Isolated infected individuals
J_T	Hospitalised infected individuals
R	Removed individuals
A	Disease awareness (auxiliary variable)

removals due to recovery or death. Table I summarises the definition of all state variables.

We use the auxiliary variable A to represent awareness of the disease. Awareness is based on available information: known (detected) cases, hospitalisations and deaths from the disease. In the case of COVID-19, many people used personal protection equipment and practiced social distancing when they became aware of the presence of the disease. This was further reinforced by stringent social distancing and confinement measures imposed or recommended by authorities. However, even if they are aware of the presence of the disease and with strong or even coercive governmental policies, not all individuals follow public health recommendations or orders. We therefore assume that susceptible individuals become educated (and therefore follow public health recommendations) at the rate

$$e(A) = \frac{e_0 A^2}{A^{*2} + A^2},$$

giving a Hill functional form [11] and described in [12, 13]. Here A^* , is the awareness level producing half of the maximum education response e_0 to campaign efforts; see [11, 14] for more details.

We model individuals flow between different compartments using the following system of differential equations

$$S' = -\lambda S - e(A)S \tag{1a}$$

$$E' = e(A)S - (1 - \varepsilon)\lambda E \tag{1b}$$

$$I'_S = \lambda S - (\alpha + e(A) + \delta)I_S \tag{1c}$$

$$I'_E = (1 - \varepsilon)\lambda E + e(A)I_S - (\alpha + \delta)I_E \tag{1d}$$

$$J'_D = (1 - \theta)\alpha(I_S + I_E) - (\gamma_1 + w)J_D \tag{1e}$$

$$J'_T = \theta\alpha(I_S + I_E) - \gamma_2 J_T + wJ_D \tag{1f}$$

$$R' = \delta(I_E + I_S) + \gamma_1 J_D + \gamma_2 J_T \tag{1g}$$

$$A = J_D + (1 + p\gamma_2)J_T, \tag{1h}$$

with initial conditions

$$(S_0, E_0, I_{S0}, I_{E0}, J_{D0}, J_{T0}, R_0) \in \mathbb{R}_+^7.$$

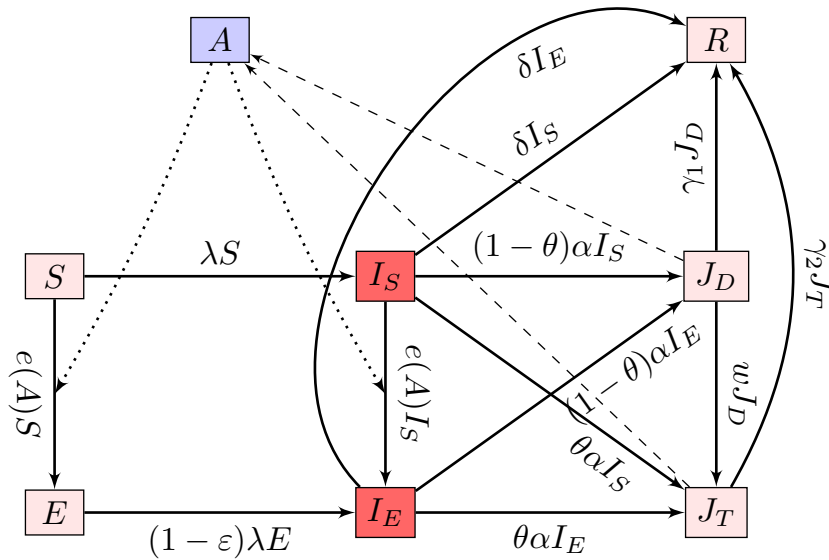


Fig. 1: Flow diagram of the model. Dark red compartments are infectious, blue represents awareness. Plain arcs are flows of individuals between compartments, dashed lines indicate the influence of compartments on *A*, dotted lines show the flows on which *A* acts.

The force of infection takes the form

$$\lambda = \beta \frac{I_S + (1 - \varepsilon)I_E}{N},$$

where β is the *per capita* transmission rate per unit time, $\varepsilon \in [0, 1]$ is the efficacy of self-protective measures, α is the detection rate and θ is the treatment rate. Table II summarises the parameters used.

Table II: Definition of parameters.

Param.	Definition
β	Transmission rate
α	Detection rate
δ	Natural recovery rate
θ	Proportion of individuals needing hospitalisation after detection
γ_1	Recovery rate for individuals in self-isolation
γ_2	Removal rate for individuals under treatment
w	Hospitalisation rate for self-isolating individuals
p	Proportion of deaths among removed individuals
A^*	Burden level producing half maximum of education response
e_0	Maximum of education response
ε	Efficacy of self-protective means

Let us briefly comment on some characteristics of the model. In a standard way as in [11], one can show that system (1) is well-posed and has a unique positive solution whenever the initial condition is positive. By

construction, the total population $N = S + E + I_S + I_E + J_D + J_T + R$ is constant.

The disease-free equilibrium (DFE) is

$$x^* = (N, 0, 0, 0, 0, 0, 0)$$

and at x^* awareness is $A = 0$ and thus $e = 0$. To apply the next generation matrix method [15], we focus on the infected compartments. Although still infected, individuals in J_D and J_T no longer contribute to the infection and can be considered as having been removed. As a consequence, the infected compartments considered for the computation are I_S and I_E . We get

$$\mathcal{F} = \begin{pmatrix} \lambda S \\ (1 - \varepsilon)\lambda E \end{pmatrix} \text{ and } \mathcal{V} = \begin{pmatrix} (\alpha + e + \delta)I_S \\ -eI_S + (\alpha + \delta)I_E \end{pmatrix}.$$

Therefore, the next generation matrix near x^* is FV^{-1} , where

$$F = \begin{pmatrix} \beta & (1 - \varepsilon)\beta \\ 0 & 0 \end{pmatrix} \text{ and } V = \begin{pmatrix} \alpha + \delta & 0 \\ 0 & \alpha + \delta \end{pmatrix}.$$

Hence, the basic reproduction number for (1) is given by

$$\mathcal{R}_0 = \rho(FV^{-1}) = \frac{\beta}{\alpha + \delta},$$

where $\rho(\cdot)$ is the spectral radius. Using the method in [16], it is also possible to derive a final size relation.

III. PARAMETER ESTIMATION AND NUMERICAL SIMULATIONS

A. Parameter estimation

We now estimate the parameters that are used in numerical simulations. First, let us establish the initial conditions used. We take the initial time to be 8 December 2019, when the first known patient developed symptoms of COVID-19 [2]. The initial susceptible population is 1.438 billion, the estimated total population of China at the time [17]. At this very early stage of the pandemic, people did not yet know about the disease and had thus not changed their behaviour to use adequate self-protection measures. Thus, initially, the educated compartments E_0 and I_{E0} are empty. Also, there were no reported recoveries or deaths of the new disease [2]. Table III summarises the initial conditions considered for (1) in simulations.

Table III: Initial conditions on 8 December 2019 (B stands for billion).

Compartment	S_0	E_0	I_{S0}	I_{E0}	J_{D0}	J_{T0}	R_0
Value	1.438B	0	1	0	1	0	0

Sequencing of the SARS-CoV-2 genome was accomplished early on, in January 2020, and as a consequence, PCR tests followed in the same month. However, because of limitations in test processing capacities, many jurisdictions, including China, have, at least at times, imposed criteria that individuals had to satisfy in order to be tested.

During the period considered, in China and Wuhan in particular, two different sets of criteria were used [18–21]. Most of the time, a *restrictive* set of criteria was in effect, requiring individuals to show many symptoms in order to be considered as suspected cases and therefore be eligible for testing, leading to what we also refer to as *normal screening*. During this period, we use the detection rate α_r . Then, between 12 and 19 February 2020, the criteria for screening were temporarily changed from the restrictive set to a *milder* set requiring less symptoms, implying that far more tests were carried out. During that short time period of *intense screening*, we use the detection rate $\alpha_m \geq \alpha_r$.

Almost all parameters in the model are fitted. However, for the proportion of deaths among removed individuals, we use the estimation in [22], namely, 0.04. To estimate parameters, we use data on cases in China between 22 January 2020 and 29 June 2020 as reported in [22]. We use the Python *Optimize Module* to fit our

model to cumulative and active cases (see Figure 2) and calibrate the parameters. Note that for active cases, this means we fit $J_D(t) + J_T(t)$. Table IV presents the parameter values found by that process.

Table IV: Parameter values found by fitting.

Parameter	Value	Remark/Source
β	0.347	Fitted
(α_r, α_m)	(0.1, 0.274)	Fitted as a step function
δ	0.058	Fitted
θ	0.023	Fitted
γ_2	0.092	Fitted
γ_1	9.16×10^{-6}	Fitted
p	0.04	[22]
ε	0.662	Fitted
w	0.099	Fitted
e_0	0.389	Fitted
A^*	36432.82	Fitted

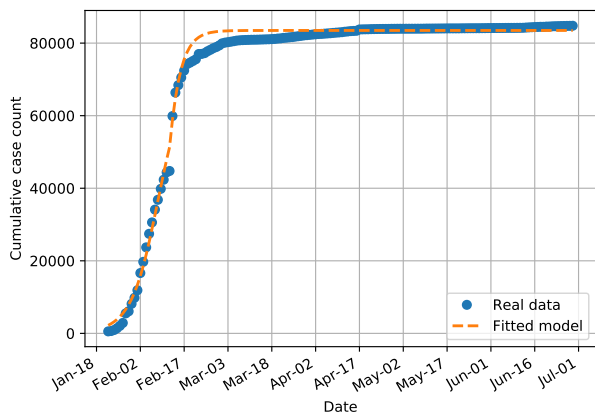
The transmission rate obtained is 0.347 day^{-1} , which is close to the mean value estimated in [23]. The time between infection and detection is calibrated to be $\alpha_r^{-1} = 10$ days, while the value $\alpha_m^{-1} = 3.649$ days is found during the intense screening period between 12 and 19 February 2020. The present study suggests a hospitalisation rate of $w = 0.099$ for 98% of detected individuals, while the remaining detected individuals go directly to hospitals, which is consistent with the results in [1], where the authors conclude that most patients were hospitalised after at least 5 days and that this delay can go up to 14 days. On the other hand, [10] reports an average recovery time after symptoms onset of 24.7 days and the mean time to death to be 17.8 days, while our fitting suggests a mean period between detection and hospital discharge by recovery or death of

$$\frac{\gamma_1}{(\gamma_1 + w)^2} + \frac{w}{\gamma_1 + w} \left(\frac{1}{\gamma_1 + w} + \frac{1}{\gamma_2} \right) = 20.832 \text{ days}$$

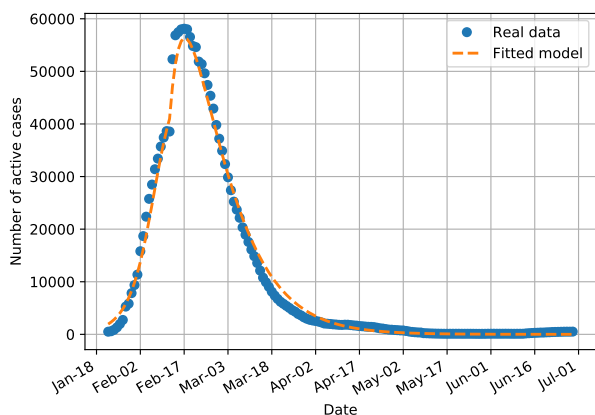
for 98% of detected individuals and $1/\gamma_2 = 10.86$ days for 2% of detected individuals, finally obtaining a mean time from detection to removal of 20.632 days. Using parameter values in Table IV, the basic reproduction number is estimated to be $\mathcal{R}_0 = 2.118$, close to the value 2.2 obtained in [1].

B. Numerical simulations

Figure 2 shows the evolution of the cumulative number and number of active cases reported by the Chinese government from 22 January to June 29 2020, as well as the result of fitting model (1) to this data, displaying good agreement with the real data. Overall, our simulation results are in accordance with both real data and published findings. We obtained that



(a) Cumulative cases



(b) Active cases

Fig. 2: Actual data and fitted solution from 22 January to 29 June 2020. Dots are the real data and dotted lines are obtained from simulations. (a) cumulative number of reported cases; (b) active reported cases.

the *per capita* per day transmissibility rate is about $\beta = 0.346 \text{ days}^{-1}$, giving a basic reproduction number of $\mathcal{R}_0 = 2.11$. The obtained values are fairly consistent with the approximations in [1].

Figure 3 shows the percentage of undetected infected individuals (including asymptomatic, mild and symptomatic individuals) among the total number of COVID-19 cases. We observe, in the beginning, an increase of the percentage of undeclared infected individuals, reaching 66% during the outbreak and remaining above 50% until 3 February 2020. This significant percentage ensured that infection continued despite the isolation of detected cases, explaining in part the persistence of transmission of COVID-19 during the early stages of the epidemic.

To get more insight into the impact of the screening protocol change, we investigate the effect of the timing

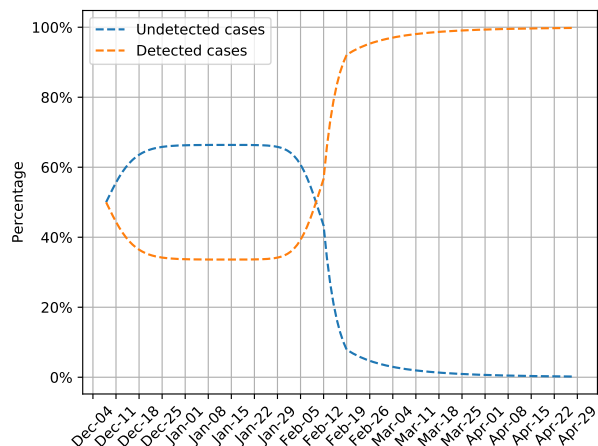
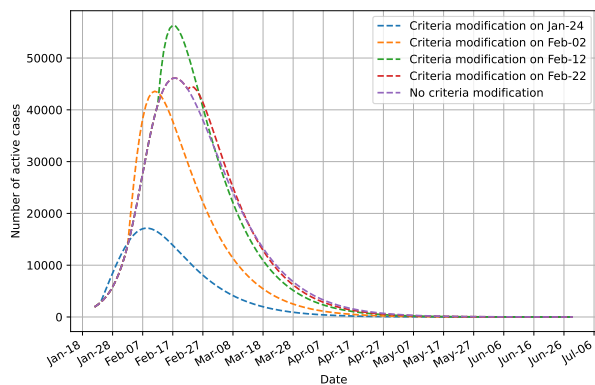


Fig. 3: Percentage repartition of undetected and detected infected individuals among the total number of infected individuals.

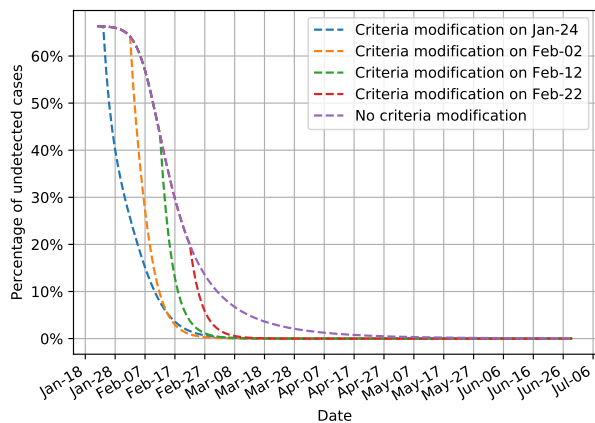
of the modification of that protocol on the intensity of the COVID-19 outbreak as shown in Figure 4. We use the parameter values in Table IV, but use α_r until the day of the modification and α_m afterwards.

We observe that the sooner we adopt a less stringent set of symptoms needed to trigger testing, the lower the percentage of undetected infected individuals, leading to a reduction of outbreak intensity. Figure 4a shows that the timing of screening criteria change strongly affects the burden of the disease. A change on 22 January 2020, for instance, leads to a burden equal to about a third of the burden that is observed when no change in screening criteria occur. This fact is explained by Figure 4b, where, with policy change on 22 January, the percentage of hidden infected individuals declines immediately and exponentially, while it does not with criteria modification on 12 February. This implicitly confirms that the presymptomatic period contains hidden infectious individuals who contributed to the persistent transmission in the early stages of the COVID-19 epidemic. We furthermore deduce that increasing the detection rate α early substantially helps to control the COVID-19 epidemic. On the contrary, we observe that a late screening intensity increase after 12 February does not have remarkable effects in dampening the disease intensity. This might be due to behavioural changes of individuals or effectiveness of preventive measures.

Figures 5, 6 and 7 address the sensitivity of the dynamics of the COVID-19 outbreak to the rate α of detection and the efficiency ε of self-protective measures. We assume no change in the screening strategy; other parameter values are taken from Table IV. In Figure 5,



(a) Active cases



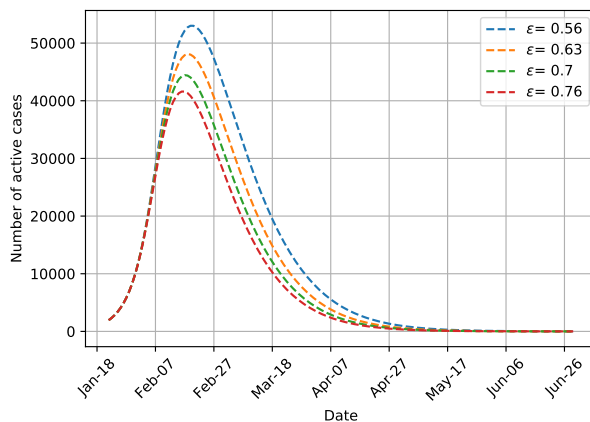
(b) Percentage undetected cases

Fig. 4: Effect of the timing of the relaxation of the criteria for screening, i.e., of the change from α_r to α_m . All dates in 2020. (a) Number of detected active cases. (b) Percentage of undetected cases among infected individuals.

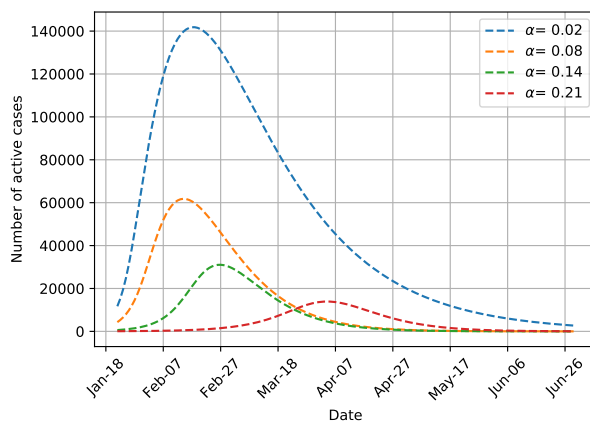
we observe that the outbreak peak is very sensitive to parameters α and ε . Figure 6a and 7a show how serious the epidemic would be with a low detection rate (see near the ε axis). Figure 6b is a zoom of Figure 6a, around the region in the (ε, α) -space close to the fitted parameters for China. This confirms that the parameters found lie in a region where solutions are quite sensitive to parameter variations, confirming the significant sensitivity to parameter α observed in Figure 5.

IV. DISCUSSION

In this work, we present a simple model for the spread of COVID-19 taking into account undetected cases, the isolation of detected cases and education favouring the use of protective measures. We fitted this model to Chinese data corresponding to the period from



(a) Sensitivity to ε

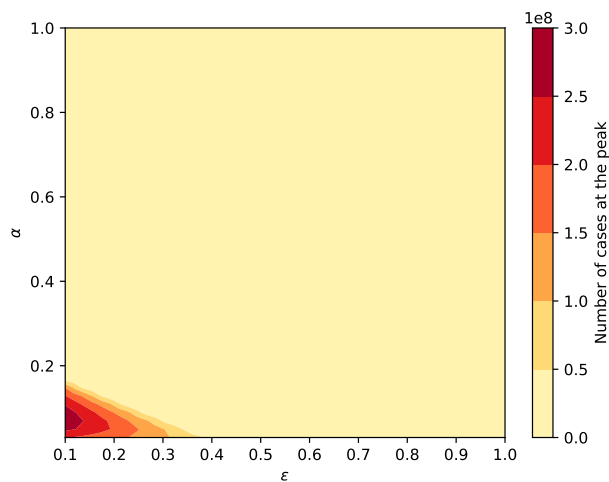


(b) Sensitivity to α

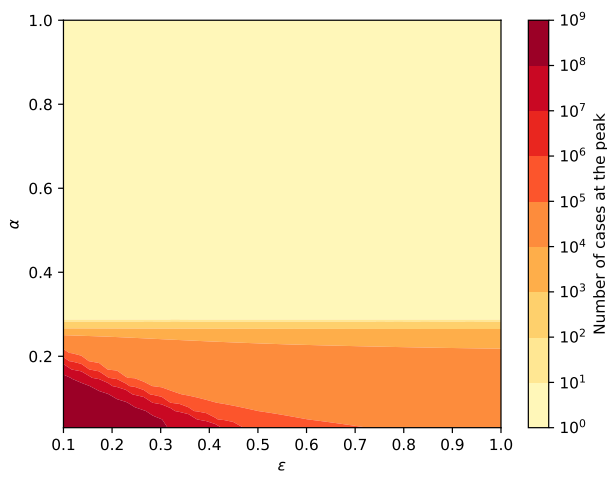
Fig. 5: Number of active cases when (a) the efficiency ε of protective measures and (b) detection rates α vary, with all other parameters as in Table IV. All dates in 2020.

the start of the epidemic to the end of June 2020. The model does a good job of fitting that data, as can be seen in Figure 2. In order to obtain this fit, though, we introduced two different values of the intensity α of screening: α_m for a period of intense screening corresponding to a loose definition of symptoms required for screening and α_r for a period with more restrictive set of symptoms leading to lower testing rates. The calibrated value $\alpha_m = 0.438$ is consistent with the results in [18–21] reporting the enhancement of the detection process on 12 February.

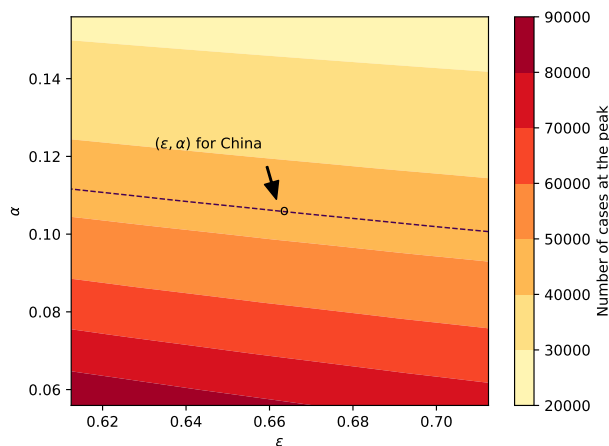
Taking the calibrated values, we then explore in more detail the effect of changing the intensity of screening. We saw in Figure 3 that stringent criteria for screening giving a detection parameter $\alpha_r = 0.17$ led to an extended time period during which over 54% of the infected individuals evaded detection. These



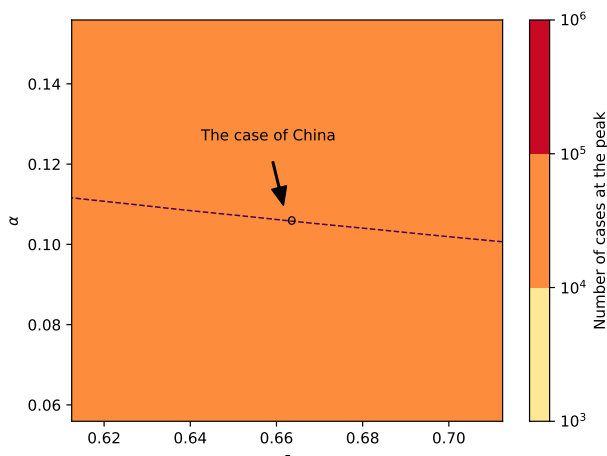
(a) Sensitivity to ϵ and α



(a) Sensitivity to ϵ and α (Logarithmic scale)



(b) Zoom around parameters found for China



(b) Zoom around parameters found for China

Fig. 6: Sensitivity of the number of active infected cases at the peak to the detection rate α and efficacy ϵ of protective measures.

Fig. 7: Sensitivity of the number of active infected cases at the peak to the detection rate α and efficacy ϵ of protective measures (Logarithmic scale).

undetected infectious individuals may not know about their infection and keep interacting with the population causing new cases even among loved ones [8]. Figure 4 strengthens the findings of Figure 3 and emphasises the effect of detection strategy change. Thus, the requirement that individuals show a large number of symptoms in order to be tested might have contributed to a longer persistence of the outbreak in China.

Interestingly, modification of screening intensity after 12 February 2020 does not have much effect (Figure 4). This may be because, as the epidemic was well established at the time, public awareness of the crisis had increased concomitantly with an expansion of the set of public protection measures, leading to an increase in

uptake of a wider variety of measures.

Besides detecting infected individuals before illness onset and isolating them, thereby reducing the chance of transmission of the disease to susceptible individuals, reporting the real number of infected individuals alerts the population about the actual danger presented by the disease. This means that more individuals, including undetected infected individuals, change their behaviour and consider all possible actions to protect themselves or others from the infection. Figure 5 considers the sensitivity of the COVID-19 outbreak dynamics to the efficacy of self-protective measures and detection rates, when these parameters are near the parameter values found for China. It shows that the outbreak is

sensitive to both parameters, with a particularly marked sensitivity to α , the rate of detection. The contour plot in Figure 6 confirms this: movement along the (self-protective measures) ε axis induces less variation than movement along the (detection) α axis.

Altogether, this highlights that good detection, for instance by deploying more tests in highly affected areas and using strategies favouring the tracing of infected individuals, has a significant effect on early spread. According to figure 6, this provides more capacity to control spread than behavioural changes and efficacy of protective measures whose use is made obligatory when detection rates are low. It would be interesting to study an optimal control problem considering the combination of the different types of interventions used here.

REFERENCES

- [1] Q. Li, X. Guan, P. Wu, X. Wang, L. Zhou, Y. Tong, et al., "Early Transmission Dynamics in Wuhan, China, of Novel Coronavirus-Infected Pneumonia", *New England Journal of Medicine*, 382(13):1199-1207, 2020.
- [2] Z. Wu, J. M. McGoogan, "Characteristics of and Important Lessons From the Coronavirus Disease 2019 (COVID-19) Outbreak in China: Summary of a Report of 72 314 Cases From the Chinese Center for Disease Control and Prevention", *JAMA*, 323(13):1239-1242, 2020.
- [3] J. Arino, "Describing, Modelling and Forecasting the Spatial and Temporal Spread of COVID-19: A Short Review", *Mathematics of Public Health*, Fields Institute Communications, 85:25-51, Springer, Cham, 2022.
- [4] P. Wu, X. Hao, E. H. Y. Lau, J. Y. Wong, K. S. M. Leung, J. T. Wu, et al., "Real-time tentative assessment of the epidemiological characteristics of novel coronavirus infections in Wuhan, China, as at 22 January 2020", *Eurosurveillance*, 25(3), 2020.
- [5] S. Zhao, Q. Lin, J. Ran, S. S. Musa, G. Yang, W. Wang, et al., "Preliminary estimation of the basic reproduction number of novel coronavirus (2019-nCoV) in China, from 2019 to 2020: A data-driven analysis in the early phase of the outbreak", *International Journal of Infectious Diseases*, 92:214-217, 2020.
- [6] C. Anastassopoulou, L. Russo, A. Tsakris, C. Siettos, "Data-based analysis, modelling and forecasting of the COVID-19 outbreak", *PLoS ONE*, 15(3):e0230405, 2020.
- [7] Y. Bai, L. Yao, T. Wei, F. Tian, D.-Y. Jin, L. Chen, M. Wang, "Presumed Asymptomatic Carrier Transmission of COVID-19", *JAMA*, 323(14):1406-1407, 2020.
- [8] P. Li, J.-B. Fu, K.-F. Li, J.-N. Liu, H.-L. Wang, L.-J. Liu, et al., "Transmission of COVID-19 in the terminal stages of the incubation period: A familial cluster", *International Journal of Infectious Diseases*, 96:452-453, 2020.
- [9] K. El Hail, M. Khaladi, A. Ouhinou, "Early-confinement strategy to tackling COVID-19 in Morocco; a mathematical modelling study", *RAIRO-Operations Research*, 56(6):4023-4033, 2022.
- [10] R. Verity, L. C. Okell, I. Dorigatti, P. Winskill, C. Whittaker, N. Imai, et al., "Estimates of the severity of coronavirus disease 2019: a model-based analysis", *The Lancet Infectious Diseases*, 20(6):669-677, 2020.
- [11] S. M. Kassa, A. Ouhinou, "Epidemiological models with prevalence dependent endogenous self-protection measure", *Mathematical Biosciences*, 229(1):41-49, 2011.
- [12] L. W. Green, A. L. McAlister, "Macro-Intervention to Support Health Behavior: Some Theoretical Perspectives and Practical Reflections", *Health Education Quarterly*, 11(3):323-339, 1984.
- [13] L. W. Green, J. M. Ottoson, C. García, R. A. Hiatt, "Diffusion Theory and Knowledge Dissemination, Utilization, and Integration in Public Health", *Annual Review of Public Health*, 30:151-174, 2009.
- [14] S. M. Kassa, A. Ouhinou, "The impact of self-protective measures in the optimal interventions for controlling infectious diseases of human population", *Journal of Mathematical Biology*, 70:213-236, 2015.
- [15] P. van den Driessche, J. Watmough, "Reproduction numbers and sub-threshold endemic equilibria for compartmental models of disease transmission", *Mathematical Biosciences*, 180(1-2):29-48, 2002.
- [16] J. Arino, F. Brauer, P. van den Driessche, J. Watmough, J. Wu, "A final size relation for epidemic models", *Mathematical Biosciences & Engineering*, 4(2):159-175, 2007.
- [17] Worldometer, China Population, <https://www.worldometers.info/world-population/china-population/>, 2020, [24/01/2023].
- [18] National Health Commission of the People's Republic of China, Interpretation of new diagnostic and treatment program for coronavirus pneumonia, 2020, <http://www.nhc.gov.cn/yzygj/s7652m/202002/54e1ad5c2aac45c19eb541799bf637e9.shtml>, [24/01/2023].
- [19] National Health Commission of the People's Republic of China, Update on new coronavirus pneumonia situation as of 24:00 on February 13, 2020, <http://www.nhc.gov.cn/yjbs7860/202002/553ff43ca29d4fe88f3837d49d6b6ef1.shtml>, [24/01/2023].
- [20] World Health Organization, Press conference on February 13, 2020, <https://twitter.com/WHO/status/1227980048952463360>, [24/01/2023].
- [21] World Health Organization, Report of the WHO-China Joint Mission on Coronavirus Disease 2019 (COVID-19), 2020, <https://www.who.int/docs/default-source/coronaviruse/who-china-joint-mission-on-covid-19-final-report.pdf>, [24/01/2023].
- [22] Worldometer, Coronavirus statistics in China, <https://www.worldometers.info/coronavirus/country/china>, [24/01/2023].
- [23] C. GU, W. Jiang, T. Zhao, B. Zheng, "Mathematical Recommendations to Fight Against COVID-19", Available at SSRN 3551006, 2020.